



Molecular beam epitaxial growth of Bi₂Se₃ nanowires and nanoflakes

G. M. Knebl, J. R. Gessler, M. Kamp, and S. Höfling

Citation: *Applied Physics Letters* **105**, 133109 (2014); doi: 10.1063/1.4896966

View online: <http://dx.doi.org/10.1063/1.4896966>

View Table of Contents: <http://scitation.aip.org/content/aip/journal/apl/105/13?ver=pdfcov>

Published by the [AIP Publishing](#)

Articles you may be interested in

[Thickness and growth-condition dependence of in-situ mobility and carrier density of epitaxial thin-film Bi₂Se₃](#)
Appl. Phys. Lett. **105**, 173506 (2014); 10.1063/1.4900749

[Two-step growth of high quality Bi₂Te₃ thin films on Al₂O₃ \(0001\) by molecular beam epitaxy](#)
Appl. Phys. Lett. **102**, 171906 (2013); 10.1063/1.4803717

[Single domain Bi₂Se₃ films grown on InP\(111\)A by molecular-beam epitaxy](#)
Appl. Phys. Lett. **102**, 151604 (2013); 10.1063/1.4802797

[Molecular beam epitaxy of high structural quality Bi₂Se₃ on lattice matched InP\(111\) substrates](#)
Appl. Phys. Lett. **102**, 041914 (2013); 10.1063/1.4789775

[Nucleation and coalescence effects on the density of self-induced GaN nanowires grown by molecular beam epitaxy](#)
Appl. Phys. Lett. **98**, 071913 (2011); 10.1063/1.3555450



Molecular beam epitaxial growth of Bi₂Se₃ nanowires and nanoflakes

G. M. Knebl,^{1,a)} J. R. Gessler,¹ M. Kamp,¹ and S. Höfling^{1,2}

¹*Technische Physik and Wilhelm Conrad Röntgen Research Center for Complex Material Systems Universität Würzburg, Am Hubland, D-97074 Würzburg, Germany*

²*SUPA, School of Physics and Astronomy, University of St Andrews, St Andrews KY16 9SS, United Kingdom*

(Received 14 August 2014; accepted 17 September 2014; published online 1 October 2014)

Topological Insulators are in focus of immense research efforts and rapid scientific progress is obtained in that field. Bi₂Se₃ has proven to be a topological insulator material that provides a large band gap and a band structure with a single Dirac cone at the Γ -point. This makes Bi₂Se₃ one of the most promising three dimensional topological insulator materials. While Bi₂Se₃ nanowires and nanoflakes so far were fabricated with different methods and for different purposes, we here present the first Bi₂Se₃ nanowires as well as nanoflakes grown by molecular beam epitaxy. The nanostructures were nucleated on pretreated, silicon (100) wafers. Altering the growth conditions nanoflakes could be fabricated instead of nanowires; both with high crystalline quality, confirmed by scanning electron microscopy as well as transmission electron microscopy. These nanostructures have promise for spintronic devices and Majorana fermion observation in contact to superconductor materials.

© 2014 AIP Publishing LLC. [<http://dx.doi.org/10.1063/1.4896966>]

In the last years, topological insulators (TIs) and new Hall states have attracted a paramount of theoretical, experimental, and material-scientific attention for the most various materials and applications.^{1–15} Bi₂Se₃ is a long known and studied thermoelectric material,^{16,17} but it has just recently been proposed to be a three dimensional topological insulator.¹⁸ Angle resolved photo electron spectroscopy showed the single Dirac cone at the Γ -point and it is 0.3 eV bandgap.¹⁹ This large band gap makes Bi₂Se₃ promising for room temperature applications in non-dissipative electronics and spintronics as well as a candidate material for topological quantum computation utilizing Majorana fermions.^{20–22} First transport measurements on ultra-thin structures indeed indicate the existence of topologically protected surface states.²³ Bulk states, however, still complicate the observation of the unique signatures of the surface states. Therefore, nanostructures provide an ideal geometric prerequisite to suppress bulk effects, as they offer a high surface to volume ratio. With rising surface to volume ratio the contribution of the bulk conductivity decreases with respect to the share of the surface states. The calculated properties of Bi₂Se₃ nanowires are described in Ref. 24.

Fabrication of Bi₂Se₃ layers was realized by different methods: pulsed laser deposition,²⁵ hot wall epitaxy,²⁵ and molecular beam epitaxy (MBE).^{23,26,27} Bi₂Se₃ nanowires, -flakes and -ribbons were synthesized so far by a variety of approaches, but mainly for thermoelectric application. Since the need of high quality samples for TI application occurred, the feasibility of nanowire, -flake and -ribbon fabrication with molecular organic chemical vapor deposition (MOCVD)²⁸ and in a horizontal tube furnace^{29,30} was shown. At very low temperatures ($T < 2.5$ K), quantum transport properties of surface states could be examined in Bi₂Se₃ nanowires fabricated in a sealed quartz tube already.³¹ Better control over growth conditions, less contamination and so higher crystal quality should enable the realization of higher temperature application

of Bi₂Se₃, for which molecular beam epitaxy is a very promising approach.

In this paper, we show the fabrication of Bi₂Se₃ nanowires as well as nanoflakes by MBE on silicon substrates. Main advantage of the MBE is the fabrication in ultra-high vacuum, minimizing the contamination. Furthermore, the high degree of control over the growth conditions, most notably the tunable Selenium to Bismuth ratio, offers opportunities for different growth regimes where the composition and crystal structure of the nanowires may be altered. Controllable fabrication of topological insulator nanostructures can enable the explicit proof of Majorana bound states. Tunnel spectroscopy on proximity induced topological superconducting nanowires are expected to show a quantized zero-bias peak and the superconducting gap that should exhibit a closing at the phase transition between topological and non-topological phase.²⁰

The fabrication was carried out with a modified Varian MBE-360. In the actual setup only two cell ports were utilized—one each with elementary Bismuth (Alfa Aesar, 99.9997%) and elementary Selenium (Alfa Aesar, 99.999 + %). The Silicon (100) wafers were pretreated before mounting. For nanowire fabrication, they were etched in hydrofluoric acid for ten seconds and then coated with a two nanometer thick layer of gold. Directly before being transferred into the MBE chamber, the substrates were scratched with metal tweezers for nanostructure nucleation. The sample was heated up to 600 °C for 10 min and afterwards cooled down to growth temperature (450 °C \pm 10 °C). The growth step took 15 min with a beam equivalent pressure ratio $r(p_{\text{Se}}/p_{\text{Bi}}) = 23$. The growth was carried out with no substrate rotation. For nanoflake fabrication the two nanometers of gold were absent. The remaining procedure for the pure nanoflake growth was equivalent to the nanowire growth.

The nanowires and nanoflakes were characterized by X-ray diffraction (XRD), scanning electron microscopy (SEM), as well as transmission electron microscopy (TEM, FEI Titan 80–300).

^{a)}gknebl@physik.uni-wuerzburg.de

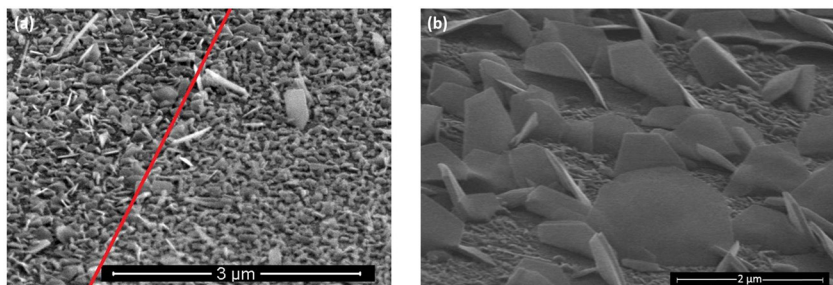


FIG. 1. Overview of: (a) Nanowire and nanoflake sample, where the left part has been scratched. The red line marks the edge of the scratch. In the scratched area and in absolute proximity to it nanowires are visible, while on the right side no wire can be found. (b) Nanoflake sample. Samples without gold show up to more than $1\ \mu\text{m}$ large Bi_2Se_3 flakes and no nanowires.

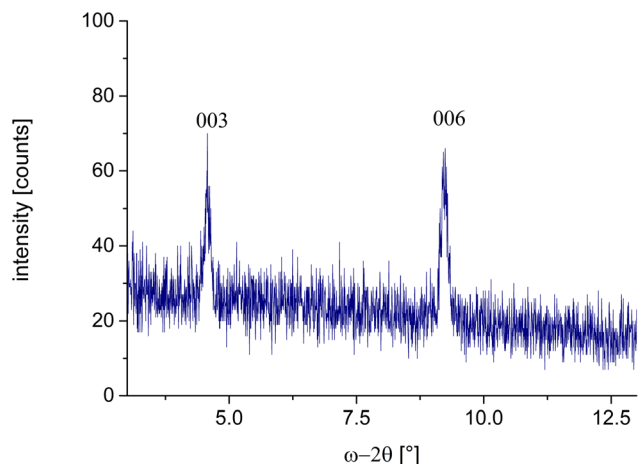


FIG. 2. XRD measurement of the as grown sample: The peaks at $\omega-2\theta = 4.6^\circ$ and $\omega-2\theta = 9.2^\circ$ correspond to the 003, respectively, 006 reflex of Bi_2Se_3 . The baseline results from the non-uniform orientation of the flakes on the surface.

The wafers pretreated with gold result in samples where the surface is covered with small nanoflakes and polycrystalline material, but in direct proximity to the scratches nanowires arise from this background. Figure 1(a) shows an overview of a scratched sample. In the upper left half, the scratched area is shown. The red line marks the edge of the scratch. While in the scratched area and in direct proximity nanowires—lighter lines—arise from the background on the wafer surface, there are no nanowires visible in distance to the scratch. For enlarged images of nanowires see Figure 3. In Figure 1(b), a sample without gold deposition is shown. Here, no nanowires occur, but outside the scratches nanoflakes with a diameter up to more than $1\ \mu\text{m}$ can be fabricated.

The material on the surface mainly consists out of Bi_2Se_3 flakes with no recognizable orientation. XRD measurements, presented in Figure 2, show clearly the 003 (at $\omega-2\theta = 4.6^\circ$) and 006 (at $\omega-2\theta = 9.3^\circ$) peak for Bi_2Se_3 . As

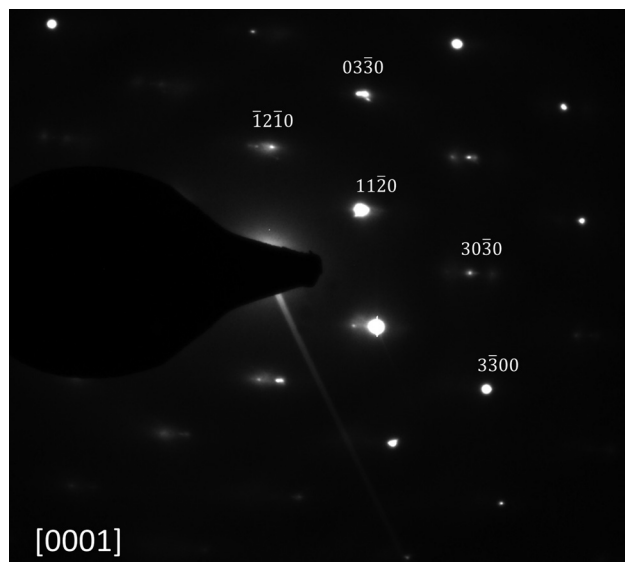


FIG. 4. Selective area diffraction pattern of a Bi_2Se_3 nanowire showing the expected hexagonal pattern.

the XRD signal originates mostly from the flakes on the wafer-surface, the blurry underground in the XRD-signal can be explained by non-uniform orientation of the flakes. SEM images, Figure 3(a), show single standing nanowires, over a covered surface. The nanowires growing out of this surface layer are enlarged in Figures 3(b) and 3(c). There are no gold droplets on the tip of the wire as it would be expected for Vapor-Liquid-Solid (VLS) growth mode.³² Typical nanowires are in a diameter of 20 nm–100 nm, an in length shorter than $1\ \mu\text{m}$.

For further, detailed examination of single wires and their crystal properties they were transferred onto a carbon grid sample holder for transmission electron microscopy. The selective area diffraction (SAD) pattern is shown in Figure 4. TEM images taken are presented in Figure 5.

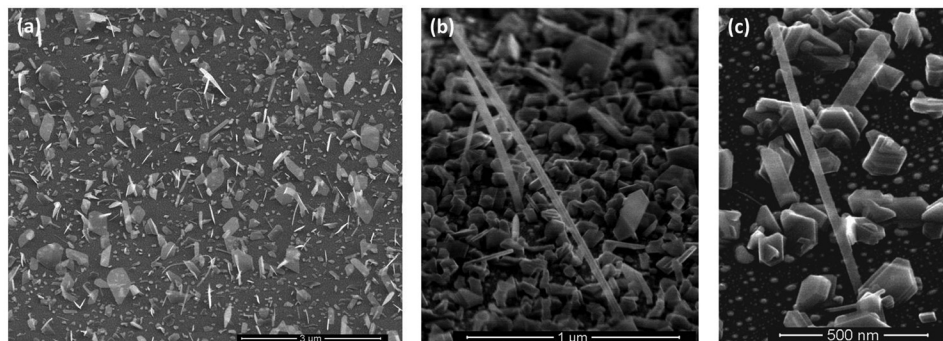


FIG. 3. (a) Bi_2Se_3 nanowires, and small nanoflakes on the surface of a gold pretreated sample near to a scratch. (b) and (c) Enlarged: single standing nanowires growing out of the flakes on the surface. On the tip of the nanowires no gold droplet can be found, indicating no vapor liquid solid growth mode.

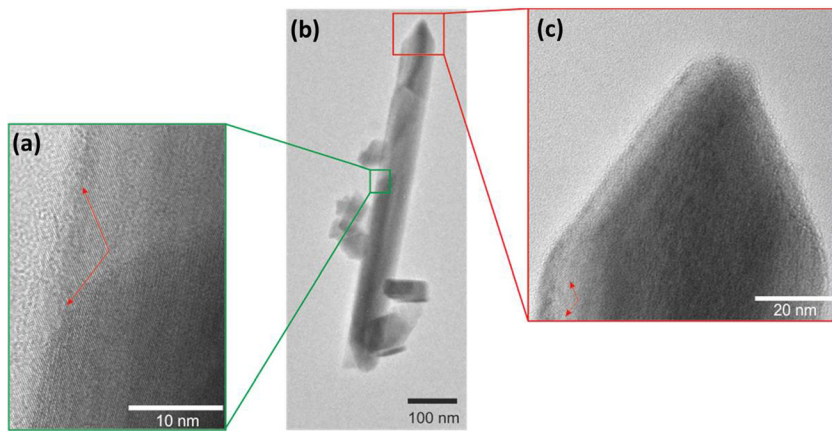


FIG. 5. High resolution TEM images showing the crystal structure of the wire: (b) nanowire and close up views of (a) an enlarged area of the sidewall of the nanowire showing clear crystal structure and (c) of an enlarged tip area of the nanowire with no gold droplet present.

Bismuth and selenium can occur in several compounds in nearly every stoichiometric combination by varying the stacking order of Bismuth and Selenium layers.³³ To validate the fabrication of Bi_2Se_3 , we here present the expected SADP for Bi_2Se_3 in Figure 4. They reveal the expected hexagonal spot pattern, indicating that the nanowires are crystalline and ordered in the rhombohedral space group $D_{3d}^5(R\bar{3}m)$.²⁸

The fabrication of crystalline Bi_2Se_3 nanowires via MBE was realized by gold and scratch pretreatment of the wafer. But the exact nucleation mechanism for our nanowire growth is not yet determined; classical VLS growth is ruled out by the fact that no gold droplets could be found on the tip of the wires, neither on SEM images in Figure 3 nor on TEM images in Figure 5.

However, nanowire growth without gold on the wafer could not be realized. Alegria *et al.* also report that the fabrication of Bi_2Se_3 nanowire fabrication by MOCVD relies on the presence of gold, but no droplets can be found on the tip of their wires.²⁸ Root catalyzed growth could not yet be found on the examined samples, but cannot be ruled out. While Kong *et al.* observed VLS grown Bi_2Se_3 nanowires by evaporating Bi_2Se_3 powder in a horizontal furnace,³⁰ our results indicate clearly the absence of VLS growth by nanowire fabrication from two atomic sources.

Further, the wires nucleate only in absolute proximity to the scratches, while in their absence no appreciable nanowire growth could be found. This fact leaves some presumptions for the nucleation mechanism; on one hand, the scratch can open defects on the wafer surface which can work as nucleation seeds. On the other hand, the material scraped off or extrinsic material brought to the wafer by the tweezers can favor the nucleation. Nanowire growth nucleated by materials different as gold is well known in literature.³⁴ Further, self-catalytic growth is known for III-V semiconductor nanowires,³⁵ in our case this means nucleation by either bismuth or selenium. So the accumulation of gold, bismuth, and/or selenium at a defect or contamination induced by the scratching step is a possible mechanism.

In conclusion, MBE is a worthwhile approach for high quality Bi_2Se_3 nanostructure fabrication on Si(100) substrates. The nanostructures shown have a mono-crystalline structure and are good candidates for further characterization as well as transport measurements. Understanding of the nanowire nucleation process can increase the wire-density and reduce

the surface coverage. Therefore, different nucleation approaches and models can be called on. As single standing nanowires on a clean substrate simplify the further processing, positioned growth on pre-patterned surface promise ideal conditions. Once completely understood MBE growth enables the implementation of further materials in the nanowires. So, e.g., $\text{Cu}_x\text{Bi}_2\text{Se}_3$ is thought to be a topological superconductor without the need of proximity induction.³⁶

We gratefully acknowledge support from the Elite Network Bavaria - international doctorate program “topological insulators” and financial support by the State of Bavaria. We thank Nadezda V. Tarakina for useful discussions on TEM analysis.

¹C. L. Kane and E. J. Mele, *Phys. Rev. Lett.* **95**, 226801 (2005).

²B. A. A. Bernevig, T. L. Hughes, and S.-C. Zhang, *Science* **314**, 1757 (2006).

³M. König, S. Wiedmann, C. Brüne, A. Roth, H. Buhmann, L. W. Molenkamp, X.-L. Qi, and S.-C. Zhang, *Science* **318**, 766 (2007).

⁴M. Hasan and C. Kane, *Rev. Mod. Phys.* **82**, 3045 (2010).

⁵J. E. Moore, *Nature* **464**, 194 (2010).

⁶X.-L. Qi and S.-C. Zhang, *Rev. Mod. Phys.* **83**, 1057 (2011).

⁷C. Liu, T. Hughes, X.-L. Qi, K. Wang, and S.-C. Zhang, *Phys. Rev. Lett.* **100**, 236601 (2008).

⁸I. Knez, C. T. Rettner, S. Yang, S. S. P. Parkin, L. Du, R.-R. Du, and G. Sullivan, *Phys. Rev. Lett.* **112**, 026602 (2014).

⁹M. Ezawa, *Phys. Rev. Lett.* **109**, 055502 (2012).

¹⁰I. Sodemann and A. H. MacDonald, *Phys. Rev. Lett.* **112**, 126804 (2014).

¹¹T. P. Kaloni, M. Tahir, and U. Schwingenschlögl, *Sci. Rep.* **3**, 3192 (2013).

¹²T. P. Kaloni, N. Singh, and U. Schwingenschlögl, *Phys. Rev. B* **89**, 035409 (2014).

¹³J. Jung and A. H. MacDonald, *Phys. Rev. B* **88**, 075408 (2013).

¹⁴Z. Qiao, W. Ren, H. Chen, L. Bellaiche, Z. Zhang, A. H. MacDonald, and Q. Niu, *Phys. Rev. Lett.* **112**, 116404 (2014).

¹⁵H. Chen, Q. Niu, and A. H. MacDonald, *Phys. Rev. Lett.* **112**, 017205 (2014).

¹⁶J. Black, E. M. Conwell, J. Seigle, and C. W. Spencer, *J. Phys. Chem. Solids* **2**, 240 (1957).

¹⁷F. D. Rosi, B. Abeles, and R. V. Jensen, *J. Phys. Chem. Solids* **10**, 191 (1959).

¹⁸H. Zhang, C.-X. Liu, X.-L. Qi, X. Dai, Z. Fang, and S.-C. Zhang, *Nat. Phys.* **5**, 438 (2009).

¹⁹Y. Xia, D. Qian, D. Hsieh, L. Wray, A. Pal, H. Lin, A. Bansil, D. Grauer, Y. S. Hor, R. J. Cava, and M. Z. Hasan, *Nat. Phys.* **5**, 398 (2009).

²⁰M. Franz, *Nat. Nanotechnol.* **8**, 149 (2013).

²¹C. Nayak, A. Stern, M. Freedman, and S. Das Sarma, *Rev. Mod. Phys.* **80**, 1083 (2008).

²²R. Hützen, A. Zazunov, B. Braunecker, A. L. Yeyati, and R. Egger, *Phys. Rev. Lett.* **109**, 166403 (2012).

²³N. Bansal, Y. S. Kim, M. Brahlek, E. Edrey, and S. Oh, *Phys. Rev. Lett.* **109**, 116804 (2012).

²⁴W.-K. Lou, F. Cheng, and J. Li, *J. Appl. Phys.* **110**, 093714 (2011).

²⁵Y. Takagaki and B. Jenichen, *Semicond. Sci. Technol.* **27**, 035015 (2012).

- ²⁶S. Schreyeck, N. V. Tarakina, G. Karczewski, C. Schumacher, T. Borzenko, C. Brüne, H. Buhmann, C. Gould, K. Brunner, and L. W. Molenkamp, *Appl. Phys. Lett.* **102**, 041914 (2013).
- ²⁷X. Guo, Z. J. Xu, H. C. Liu, B. Zhao, X. Q. Dai, H. T. He, J. N. Wang, H. J. Liu, W. K. Ho, and M. H. Xie, *Appl. Phys. Lett.* **102**, 151604 (2013).
- ²⁸L. D. Alegria, M. D. Schroer, A. Chatterjee, G. R. Poirier, M. Pretko, S. K. Patel, and J. R. Petta, *Nano Lett.* **12**, 4711 (2012).
- ²⁹D. Kong, W. Dang, J. J. Cha, H. Li, S. Meister, H. Peng, Z. Liu, and Y. Cui, *Nano Lett.* **10**, 2245 (2010).
- ³⁰D. Kong, J. C. Randel, H. Peng, J. J. Cha, S. Meister, K. Lai, Y. Chen, Z.-X. Shen, H. C. Manoharan, and Y. Cui, *Nano Lett.* **10**, 329 (2010).
- ³¹J. Dufouleur, L. Veyrat, A. Teichgräber, S. Neuhaus, C. Nowka, S. Hampel, J. Cayssol, J. Schumann, B. Eichler, O. G. Schmidt, B. Büchner, and R. Giraud, *Phys. Rev. Lett.* **110**, 186806 (2013).
- ³²R. S. Wagner and W. C. Ellis, *Appl. Phys. Lett.* **4**, 89 (1964).
- ³³H. Okamoto, *J. Phase Equilib.* **15**, 195 (1994).
- ³⁴C. Chêze, L. Geelhaar, O. Brandt, W. M. Weber, H. Riechert, S. Münch, R. Rothmund, S. Reitzenstein, A. Forchel, T. Kehagias, P. Komninou, G. P. Dimitrakopoulos, and T. Karakostas, *Nano Res.* **3**, 528 (2010).
- ³⁵B. Mandl, J. Stangl, T. Mårtensson, A. Mikkelsen, J. Eriksson, L. S. Karlsson, G. Bauer, L. Samuelson, and W. Seifert, *Nano Lett.* **6**, 1817 (2006).
- ³⁶Y. S. Hor, A. J. Williams, J. G. Checkelsky, P. Roushan, J. Seo, Q. Xu, H. W. Zandbergen, A. Yazdani, N. P. Ong, and R. J. Cava, *Phys. Rev. Lett.* **104**, 057001 (2010).